Regular Article

PHYSICAL CHEMISTRY RESEARCH
Published by the
Iranian Chemical Society
www.physchemres.org
info@physchemres.org

Phys. Chem. Res., Vol. 11, No. 4, 877-887, December 2023
DOI: 10.22036/pcr.2022.356675.2171

Adsorption of Some Gas Molecules on the Surface of Graphene Nanoflakes

M.A. Rafiei and M. Namazian*

Department of Chemistry, Yazd University, Yazd, Iran

(Received 17 August 2022, Accepted 19 December 2022)

The adsorption of some monatomic and polyatomic gases on the surface of graphene nanoflakes was investigated. The surface of graphene nanoflakes was modeled, and a suitable model was found among a set of 2, 4, 7, and 19 hexagonal rings. State-of-the-art density functional theory calculations were used in the present work. The adsorption energies and equilibrium distances were calculated for a variety of monatomic and polyatomic gases, such as Ar, O_2, CO_2, and CS_2, for all possible orientations. In this study, the following three highly symmetric adsorption sites on the surface were studied: atom-site, hollow-site, and bridge-site. The hollow-site for monatomic gases and the bridge-site for polyatomic gases (*i.e.*, CO_2 and CS_2) were found to be more favorable than other sites. The best orientation for the studied polyatomic gases was found to be parallel. The results are compared with the available experimental data.

Keywords: Graphene, Adsorption, Carbon dioxide, Carbon disulfide, Noble gas

INTRODUCTION

Graphene, a single-atom-thick two-dimensional (2D) honeycomb structure composed of carbon atoms [1], has attracted enormous attention due to its mechanical flexibility [2], electronic and thermal conductivity [3-9], and optical transparency [10]. These remarkable properties of graphene sheets could facilitate their application in a wide range of fields, such as sensing [11], electronics [12-15], energy storage [16-23], biomedicine [24-25], and catalysis [26]. In particular, graphene shows considerable potential for adsorption due to its mechanical property, easy-to-be-modified nature, and large surface area [27-28]; thus, external atoms or molecules can be easily adsorbed on its surface [29-38].

Noble gases, also known as rare gases, are widely used in industries and laboratories; accordingly, their adsorption and storage are of great importance and need to be fully understood. Oxygen (O_2) is the second most abundant gas in the atmosphere, and carbon dioxide (CO_2) and carbon disulfide (CS_2) are two common atmospheric pollutants. CO_2 is considered one of the most important greenhouse gases and the main cause of global warming. Similarly, CS_2 can react with other volatile organic substances in the air and harm the environment.

A number of theoretical studies have focused on the adsorption of gases on pristine and functionalized graphene nanoflakes. For example, regarding the adsorption of noble gases, Sheng *et al*. studied the adsorption of Xe at three high-symmetry sites on the surface of graphene [39]. Moreover, Ambrosetti *et al*. used DFT/vdW-WF method to study the adsorption of He, Ar, and Xe on graphite and graphene surfaces at three high-symmetry sites [40]. Maiga *et al.* analyzed the adsorption of Ar, Kr, and Xe on graphene using molecular simulation [41]. Vazhappilly *et al.* investigated the binding strength of Xe and Kr atoms on porous as well as various doped graphene surfaces [42]. Regarding oxygen adsorption, Zhu *et al*. studied the effects of different amounts of atomic oxygen on graphene [43]. Qu *et al.* [44] reported on the effects of equibiaxial strain on the interactions between O_2 and various graphene composites [44]. Bagsican *et al.* experimentally determined the adsorption and desorption dynamics of oxygen molecules on graphene using temperature-programmed terahertz emission microscopy

*Corresponding author. E-mail: namazian@yazd.ac.ir

[45]. Yan *et al.* analyzed the O_2 adsorption and dissociation on graphene using density functional theory (DFT) [46]. The adsorption of CO_2 on graphene has also attracted the attention of researchers. For example, Lee *et al.* analyzed the energy change for the adsorption of CO_2 on graphene using different levels of theory [47]. In addition, Osouleddini *et al.* analyzed the interaction of CO_2 and CH_4 molecules with graphene and a tetracyanoethylene-modified graphene surface by comparing the strength of their interactions [48]. Takeuchi *et al.* studied the adsorption of CO_2 on graphene by combining temperature-programmed desorption, X-ray photoelectron spectroscopy, and van der Waals density functional (vdW-DF) method [49]. Tit *et al.* performed calculations on the adsorption of CO_2 and CO on graphene [50]. They investigated the selectivity and the chemical activity of graphene in the adsorption of CO_2 and CO molecules. It is worth noting that while graphene is an infinitive 2D compound, experimental and theoretical studies have usually been carried out on the finite size of graphene surface, which is called graphene nanoflake [51-53].

Although various studies have been carried out on the adsorption of gases on graphene [39-50], to the best of our knowledge, no systematic analysis has been done on the adsorption of He, Ne, Ar, Kr, O_2, CO_2, and CS_2 molecules on graphene nanoflakes and, more specifically, their atomic/molecular configurations. The aim of the present work was to study the interaction between the aforementioned gases and monolayer graphene nanoflakes by DFT calculations. Furthermore, detailed information is provided on various configurations of approaching gases, different sites of graphene nanoflakes, equilibrium distances, levels of theory, and different models for the process of adsorption.

COMPUTATIONAL DETAILS

All DFT calculations were carried out using the ORCA 4.2.1 software package [54]. The M06-2X/6-311+G(d,p) level of theory was used for geometry optimization and calculation of relaxed or unrelaxed surface energies [55]. The M06-2X functional, which is a hybrid meta-functional and high parameterized empirical exchange-correlation functional [55], has been used in recent theoretical studies and reported to have acceptable performance for main group elements [56-60]. Moreover, the M06-2X functional gives good interaction energies for vdW complexes near equilibrium structures [61]. The basis set of 6-311+G(d,p) was reported to be appropriate for the weak physisorption on carbon-based materials [62-66].

The adsorption energy (E_{ads}), describing the interaction between the studied gases and graphene, was calculated using Eq. (1):

$$E_{ads} = E_{graphene+gas} - (E_{graphene} + E_{gas}) \quad (1)$$

where $E_{graphene+gas}$ is the total energy of the absorbed gas on graphene, $E_{graphene}$ is the energy of pristine graphene, and E_{gas} is the energy of the free gas.

Molecules were placed on a monolayer graphene, which had 7 hexagonal rings and was composed of 36 atoms in the (x,y) plane. To neutralize the valances of terminal carbons, the graphene sheet was constructed with hydrogen termination at the edges. The adsorbed molecules were set in two orientations, namely, *par* and *perp*, which stand for parallel and perpendicular to the graphene surface, respectively. As shown in Fig. 1, the following three highly symmetric adsorption positions were also studied: *A* (atom-site: over a C atom), *H* (hollow-site: at the center of a hexagonal ring), and *B* (bridge-site: over the midpoint of a C-C bond).

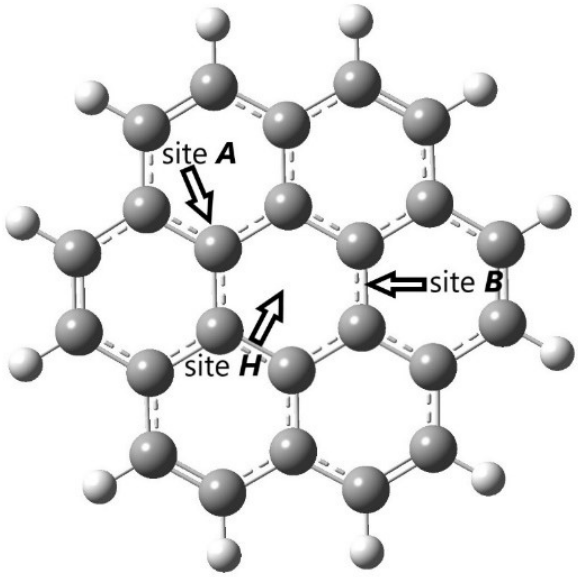

Fig. 1. Different sites of graphene nanoflakes.

RESULTS AND DISCUSSION

Modeling of Graphene and Method of Calculations

Graphene is a single-atom-thick 2D honeycomb structure composed of hexagonal rings. In this study, due to computing time and hardware limitations, only a few of its rings were considered in the chemical model of graphene. To minimize calculations, the least number of rings that could render reliable results was considered. As shown in Fig. 2, four models were investigated, which were composed of 2, 4, 7, and 19 rings.

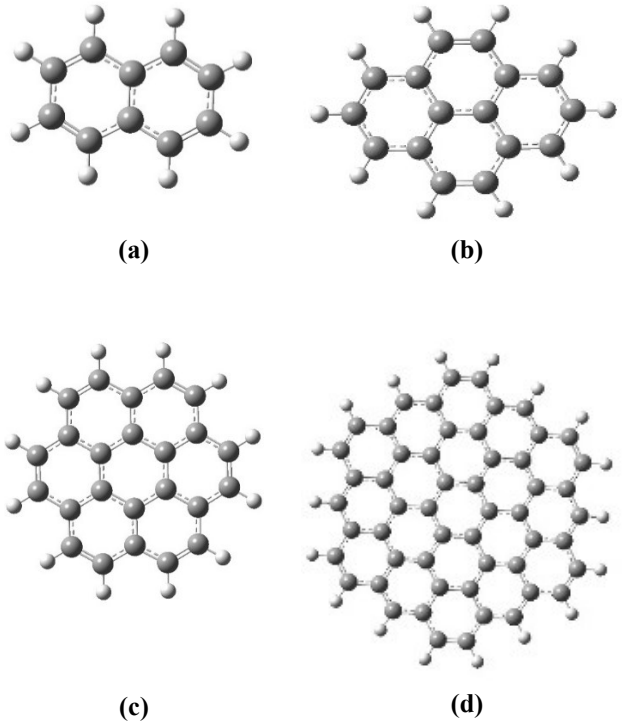

Fig. 2. Modeling of graphene nanoflakes with different numbers of rings: (a) two rings (2-R), (b) four rings (4-R), (c) seven rings (7-R), and (d) nineteen rings (19-R).

For the adsorption of Ne on the *H* site of graphene, the above four models were calculated. Table 1 summarizes the results of calculations.

As shown in Table 1, with the increase in the number of rings, the absolute value of E_{ads} also increased. For the 7-R and 19-R models, the difference between the calculated E_{ads} was only 0.1 kJ mol^{-1}. The equilibrium distances were also calculated for the above four models (Table 1). The equilibrium distances were 2.9 Å for both 7-R and 19-R models. Figure S1 (included in Supporting Information, SI) shows the variation of potential energy curves with respect to distance. The calculations were carried out for Ar noble gas, and the same results were achieved (see SI, Table S1). Based on the results, the 7-R model was found to be adequate for modeling graphene and was used for further calculations.

Table 1. Adsorption Energies (E_{ads}) and Equilibrium Distances (d_0) of Ne on the *H* Site in Graphene with Four Different Numbers of Rings: Two Rings (2-R), Four Rings (4-R), Seven Rings (7-R), and Nineteen Rings (19-R)

Number of rings	E_{ads} (kJ mol^{-1})	d_0 (Å)
2-R	-4.9	3.0
4-R	-5.5	2.9
7-R	-6.7	2.9
19-R	-6.8	2.9

The choice of functional and basis set was crucial in the calculation of physical processes. In this study, four popular functionals, including B3LYP, BMK, BH and HLYP, and M06-2X, along with a triple-ζ diffuse function basis set 6-311+G(d,p) with additional polarization functions, were employed [67]. The adsorption energies and equilibrium distances were calculated for the atom of Ne on the *H* site of graphene, and the results are presented in Table 2 and Fig. 3.

Table 2. Adsorption Energies (E_{ads}) and Equilibrium Distances (d_0) for Ne on the ***H*** Site Obtained from Different Functionals and the 6-311+G(d,p) Basis Set

Functional	E_{ads} (kJ mol^{-1})	d_0 (Å)
M06-2X	-5.7	2.9
BHandHLYP	-1.9	3.2
BMK	-0.7	5.1
B3LYP	-0.9	3.4

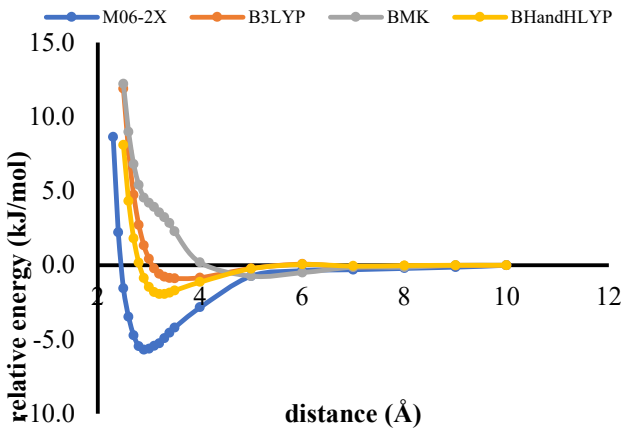

Fig. 3. Potential energy curves for the adsorption of Ne on the *H* site calculated by M06-2X, BHandHLYP, BMK, and B3LYP functionals with the 6-311+G(d,p) basis set.

As shown in Table 2, the M06-2X adsorption energy was considerably more negative than the energy values calculated by other functionals. Also, the equilibrium distance calculated by the M06-2X was remarkably shorter than other distances. To explore the effect of the basis set on the calculation of energies and equilibrium distances, the basis sets of 6-31+G(d,p), 6-311+G(d,p), 6-311+G(2df,p), and cc-pVTZ were studied, and the results are shown in Table 3 and Fig. 4.

The values presented in Table 3 show that all triple-ζ basis sets resulted in similar values. Based on the number of basis functions and the calculation time, M06-2X/6-311+G(d,p) was used for further calculations.

Adsorption of Noble Gases

The adsorption of monatomic noble gases of He, Ne, Ar, and Kr on different sites of *A*, *B*, and *H* on graphene was studied, and the results are presented in Table 4 and Fig. 5.

Based on the energy and distance values presented in Table 4, site *H* was found to be a better position compared to other sites, including *A* and *B*, for all the above-mentioned gases. Also, with the increase in the size of gases, the adsorption energies increased and the adsorption energies for He, Ne, Ar, and Kr were -3.8, -5.7, -8.0, and -9.6 kJ mol^{-1}, respectively. The increase in the adsorption energy from He to Kr was remarkable. This finding is in agreement with the fact that larger gases have stronger dipole-dipole interactions.

Table 3. Adsorption Energies (E_{ads}) and Equilibrium Distances (d_0) for Ne on the *H* Site Obtained from Different Basis Sets and the M06-2X Functional

Basis set	E_{ads} (kJ mol^{-1})	d_0 (Å)
6-311+G(2df,p)	-5.5	2.9
6-311+G(d,p)	-5.7	2.9
6-31+G(d,p)	-4.8	3.0
cc-pVTZ	-5.5	2.9

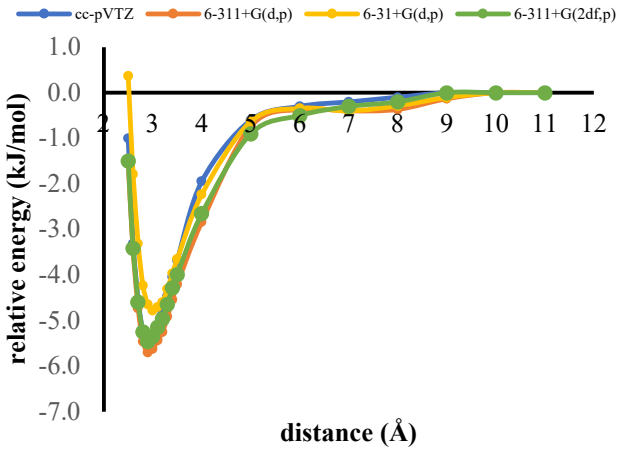

Fig. 4. Potential energy curves for the adsorption of Ne on the *H* site calculated by 6-311+G(2df,p), 6-311+G(d,p), 6-31+G(d,p), and cc-pVTZ basis sets with the M06-2X functional.

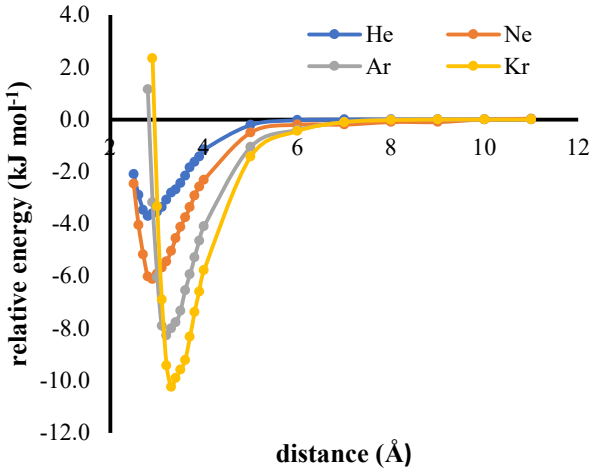

Fig. 5. Potential energy curves for the adsorption of He, Ne, Ar, and Kr on the *H* site.

Table 4. Adsorption Energies (E_{ads}) and Equilibrium Distances (d_0) for He, Ne, Ar, and Kr on Different Positions: The Molecule is on Top of a Carbon Atom (Site *A*), the Midpoint of a Carbon-Carbon Bond (Site *B*) and the Center of a Hexagon (Site *H*) (Fig. 1)

	Site *A*		Site *B*		Site *H*	
Noble gases	E_{ads} (kJ mol^{-1})	d_0 (Å)	E_{ads} (kJ mol^{-1})	d_0 (Å)	E_{ads} (kJ mol^{-1})	d_0 (Å)
He	-2.8	3.1	-3.0	3.0	-3.8	2.8
Ne	-5.6	3.0	-5.6	3.0	-5.7	2.9
Ar	-7.7	3.3	-8.0	3.3	-8.0	3.3
Kr	-9.5	3.5	-8.9	3.3	-9.6	3.3

The equilibrium distances for He, Ne, Ar, and Kr were 2.8, 2.9, 3.3, and 3.3 Å, respectively. This is also in agreement with the results of previous research [68].

Adsorption of O_2

The adsorption energies and equilibrium distances for *perp* orientation of O_2 on different sites of *A*, *B*, and *H* were calculated, and the results are presented in Table 5 and Fig. 6.

The values presented in Table 5 show that the minimum adsorption energy (*i.e.*, -12.3 kJ mol^{-1}) was obtained for site *H*. The equilibrium distance was also smaller for site *H*, which confirms that this site was more favorable than the other two sites. Adsorption energies, together with equilibrium distances, show that the order of sites for *perp* orientation was as follows: $H > A > B$.

To investigate different orientations of O_2 with respect to the surface of graphene, φ was defined as the angle of oxygen-oxygen-surface, so that φ = 90° and φ =180° presented the *par* and *perp* orientations, respectively, as shown in Fig. 7.

Table 5. Adsorption Energies (E_{ads}) and Equilibrium Distances (d_0) for the *Perp* Oxygen Molecule on Different Positions on the Surface: Site *A*, Site *B*, and Site *H*

Different sites	E_{ads} (kJ mol^{-1})	d_0 (Å)
Site *A*	-9.6	3.0
Site *B*	-9.5	3.9
Site *H*	-12.3	2.9

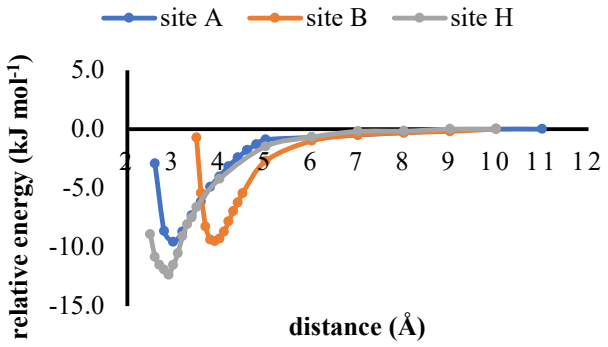

Fig. 6. Potential energy curves for the adsorption of oxygen molecules on different sites, including site *A*, site *B*, and site *H* (*perp* orientation).

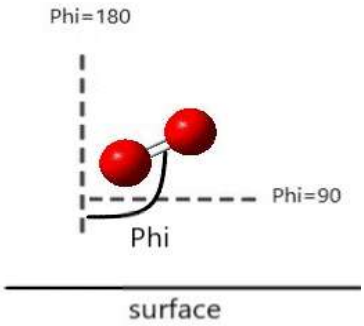

Fig. 7. The representation of the angle between the oxygen-oxygen surface (Phi).

The calculated relative adsorption energies for different values of φ are presented in Table S2, which shows that the lowest adsorption energy occurs for 90 degree or *par* orientation. These relative energies varied from 0-5 kJ mol^{-1}. It can be concluded that the best position for O_2 on graphene was a *par* orientation on the *H* site on which the adsorption energy was -13.5 kJ mol^{-1} and the equilibrium distance was approximately 3.0 Å above the surface of graphene.

Adsorption of CO_2 and CS_2

Furthermore, various configurations and equilibrium distances were studied for the adsorption of CO_2 and CS_2 on graphene. Different sites, including *A*, *B*, and *H*, were investigated for the studied orientations. Table 6 presents the adsorption energies along with the equilibrium distances.

As shown in Table 6, the lowest adsorption energies for both CO_2 and CS_2 were obtained for site *H*, but the differences between their energies were insignificant. Regarding the equilibrium distance, site *H* also showed slightly shorter distances.

For the *par* orientation, different sites, including *A*, *B*, and *H*, were also considered, and it was found that site *B* was slightly more favorable than the other two sites, as shown in Fig. 9.

This finding is in agreement with a previous report [47]. A comparison between the two orientations of *par* and *perp* for the adsorption of CO_2 and CS_2 on the surface of graphene showed that the *par* orientation was significantly better in terms of adsorption energies, as shown in Table 7. The differences between the *par* and *perp* orientations were 7-8 kJ mol^{-1} for the above two gases. A comparison of the adsorption energies of CO_2 and CS_2 for all studied orientations showed that the adsorption process was more favorable for CS_2, as can be seen in Table 7 and Fig. 10.

The calculated adsorption energies were -19.4 and -25.5 kJ mol^{-1} for CO_2 and CS_2, respectively, and the equilibrium distances were 3.0 and 3.4 Å for CO_2 and CS_2, respectively.

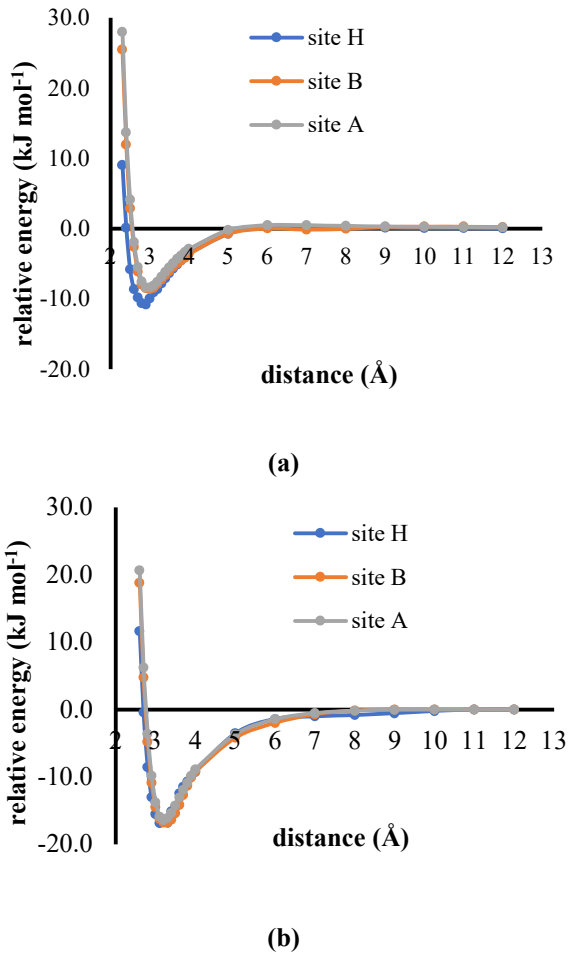

Fig. 8. Potential energy curves for the adsorption (a) *perp* CO_2 molecule and (b) *perp* CS_2 molecule on different sites, including site *A*, site *B*, and site *H*.

Table 6. Adsorption Energies (E_{ads}) and Equilibrium Distances (d_0) for *Perp* CO_2 and *Perp* CS_2 Molecules on Different Positions: Site *A*, Site *B*, Site *H*

	CO_2		CS_2	
Sites	E_{ad} (kJ mol^{-1})	d_0 (Å)	E_{ad} (kJ mol^{-1})	d_0 (Å)
A	-8.4	2.9	-16.4	3.2
B	-8.6	3	-16.7	3.2
H	-10.8	2.9	-16.8	3.1

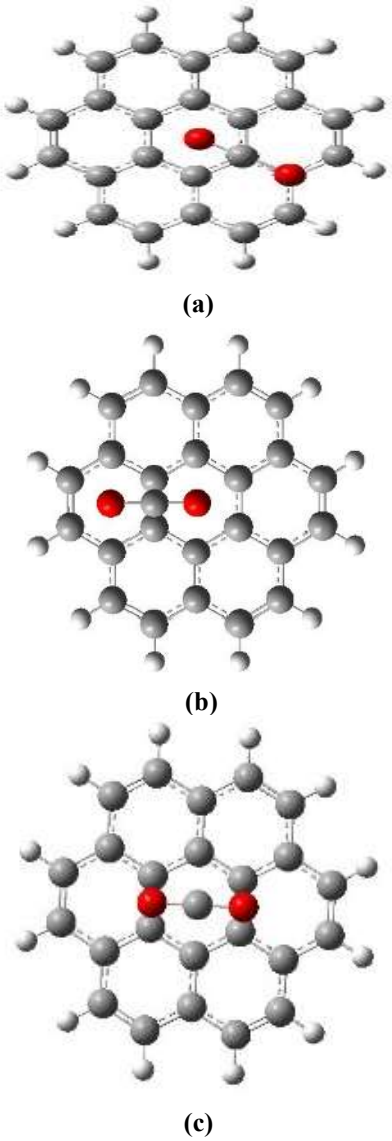

Fig. 9. The *par* situation of CO_2 and CS_2 molecules on different sites of graphene: (a) site *A*, (b) site *B*, and (c) site *H*.

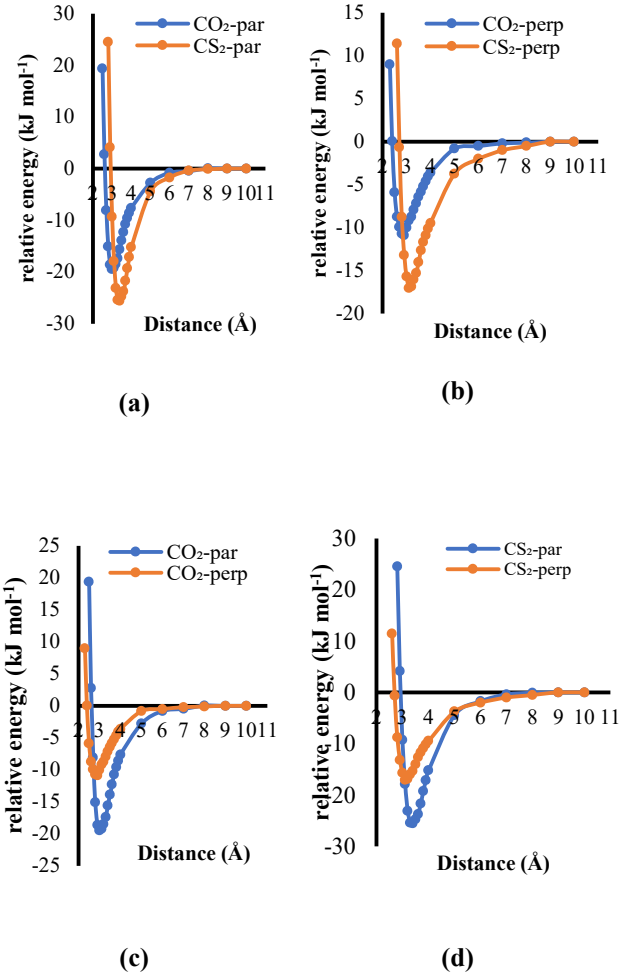

Fig. 10. Potential energy curves for the adsorption (a) *par* orientation of CO_2 and CS_2 molecules, (b) *perp* orientation of CO_2 and CS_2 molecules on the *H* site, (c) *par* and *perp* orientations of CO_2 molecule, and (d) *par* and *perp* orientations of CS_2 molecule.

Table 7. Adsorption Energies (E_{ads}) and Equilibrium Distances (d_0) for *Par* and *Perp* Orientations of CO_2 and CS_2 Molecules

	CO_2-*par*	CO_2-*perp*	CS_2-*par*	CS_2-*perp*
E_{ads} (kJ mol^{-1})	-19.4	-10.8	-25.5	-16.8
d_0 (Å)	3.0	2.9	3.4	3.1

CONCLUSIONS

In the present study, an extensive study of the adsorption of He, Ne, Ar, Kr, O_2, CO_2, and CS_2 on the surface of graphene nanoflakes was carried out and the results showed that the adsorption of all the studied gases occurred in the physical nature. Based on the results, it can be stated that a hexagonal planar 7-ring is an adequate model to characterize the graphene surface. The adsorption energies for monatomic noble gases varied in the range of -3.8 to -9.6 kJ mol^{-1}. The smallest atom of He and Kr showed the lowest and highest energy in the above range. For the diatomic molecules of O_2, the calculated adsorption energy was -13.5 kJ mol^{-1} whereas for the triatomic gases of CO_2 and CS_2, the calculated energies were -19.4 and -25.5 kJ mol^{-1}, respectively. The equilibrium distances of the studied gases, including He, Ne, Ar, Kr, O_2, CO_2, and CS_2, were 2.8, 2.9, 3.3, 3.3, 3.0, 3.0, and 3.4 Å, respectively. All different configurations and symmetric adsorption positions were investigated. For the monatomic gases and O_2, site *H* was found to be the best position whereas for the CO_2 and CS_2, site *B* was observed to be more favorable. The best orientation for the studied polyatomic gases was found to be *par* orientation.

ACKNOWLEDGEMENTS

M. R. is grateful to Yazd University for the postgraduate scholarship. The authors also would like to thank the Department of Theory and Spectroscopy, Max Planck Institute, Germany, for providing us with the open-source version of ORCA 4.2.1 (http://https://www.faccts.de/orca/).

REFERENCES

[1] Novoselov, K. S.; Geim, A. K.; Morozov, S. V.; Jiang, D. -E.; Zhang, Y.; Dubonos, S. V.; Grigorieva, I. V.; Firsov, A. A., Electric field effect in atomically thin carbon films. S*cience* **2004**, *306*, 666-669, https://doi.org/10.1126/science.1102896.

[2] Gómez-Navarro, C.; Burghard, M.; Kern, K., Elastic properties of chemically derived single graphene sheets. *Nano Lett.* **2008**, *8*, 2045-2049, https://doi.org/10.1021/nl801384y.

[3] Geim, A. K.; Novoselov, K. S., The rise of graphene. *Nanosci. Technol.* **2010**, *6*, 11-19, https://doi.org/10.1142/9789814287005_0002.

[4] Soldano, C.; Mahmood, A.; Dujardin, E., Production, properties and potential of graphene. *Carbon* **2010**, *48*, 2127-2150, https://doi.org/10.1016/j.carbon.2010.01.058.

[5] Wang, L.; Meric, I.; Huang, P.; Gao, Q.; Gao, Y.; Tran, H.; Taniguchi, T.; Watanabe, K.; Campos, L.; Muller, D., One-dimensional electrical contact to a two-dimensional material. *Science* **2013**, *342*, 614-617, https://doi.org/10.1126/science.1244358.

[6] Levy, N.; Burke, S.; Meaker, K.; Panlasigui, M.; Zettl, A.; Guinea, F.; Neto, A. C.; Crommie, M. F., Strain-induced pseudo–magnetic fields greater than 300 tesla in graphene nanobubbles. *Science* **2010**, *329*, 544-547, https://doi.org/10.1126/science.1191700.

[7] Rabchinskii, M. K.; Ryzhkov, S. A.; Kirilenko, D. A.; Ulin, N. V.; Baidakova, M. V.; Shnitov, V. V.; Pavlov, S. I.; Chumakov, R. G.; Stolyarova, D. Y.; Besedina, N. A., From graphene oxide towards aminated graphene: Facile synthesis, its structure and electronic properties. *Sci. Rep.***2020**,*10*, 1-12, https://doi.org/10.1038/s41598-020-63935-3.

[8] Huang, X.; Zhi, C.; Lin, Y.; Bao, H.; Wu, G.; Jiang, P.; Mai, Y. -W., Thermal conductivity of graphene-based polymer nanocomposites. *Mater. Sci. Eng. R Rep.* **2020**, *142*, 100577, https://doi.org/10.1016/j.mser.2020.100577.

[9] Li, M.; Zhou, H.; Zhang, Y.; Liao, Y.; Zhou, H., Effect of defects on thermal conductivity of graphene/epoxy nanocomposites. *Carbon* **2018**, *130*, 295-303, https://doi.org/10.1016/j.carbon.2017.12.110.

[10] Eda, G.; Fanchini, G.; Chhowalla, M., Large-area ultrathin films of reduced graphene oxide as a transparent and flexible electronic material. *Nat. Nanotechnol.* **2008**, *3*, 270-274, https://doi.org/10.1038/nnano.2008.83.

[11] Liu, Y.; Dong, X.; Chen, P., Biological and chemical sensors based on graphene materials. *Chem. Soc. Rev.* **2012**, *41*, 2283-2307, https://doi.org/10.1039/C1CS15270J.

[12] Lin, Y. -M.; Jenkins, K. A.; Valdes-Garcia, A.; Small, J. P.; Farmer, D. B.; Avouris, P., Operation of graphene transistors at gigahertz frequencies. *Nano Lett.* **2009**, *9*,

422-426, https://doi.org/10.1021/nl803316h.

[13] Chaban, V. V.; Prezhdo, O. V., Nitrogen-nitrogen bonds undermine stability of N-doped graphene. *J. Am. Chem. Soc.* **2015**, *137*, 11688-11694, https://doi.org/10.1021/jacs.5b05890.

[14] Dean, C. R.; Young, A. F.; Meric, I.; Lee, C.; Wang, L.; Sorgenfrei, S.; Watanabe, K.; Taniguchi, T.; Kim, P.; Shepard, K. L., Boron nitride substrates for high-quality graphene electronics. *Nat. Nanotechnol.* **2010**, *5*, 722-726, https://doi.org/10.1038/nnano.2010.172.

[15] Neto, A. C.; Guinea, F.; Peres, N. M.; Novoselov, K. S.; Geim, A. K., The electronic properties of graphene. *Rev. Mod. Phys.* **2009**, *81*, 109, https://doi.org/10.1103/RevModPhys.81.109.

[16] Pumera, M., Graphene-based nanomaterials for energy storage. *Energy Environ. Sci.* **2011**, *4*, 668-674, https://doi.org/10.1039/C0EE00295J.

[17] Jeong, H. M.; Lee, J. W.; Shin, W. H.; Choi, Y. J.; Shin, H. J.; Kang, J. K.; Choi, J. W., Nitrogen-doped graphene for high-performance ultracapacitors and the importance of nitrogen-doped sites at basal planes. *Nano Lett.* **2011**, *11*, 2472-2477, https://doi.org/10.1021/nl2009058.

[18] Wang, T.; Wang, L. -X.; Wu, D. -L.; Xia, W.; Jia, D. -Z., Interaction between nitrogen and sulfur in co-doped graphene and synergetic effect in supercapacitor. *Sci. Rep.* **2015**, *5*, 1-9, https://doi.org/10.1038/srep09591.

[19] Xu, Y.; Liu, J., Graphene as transparent electrodes: fabrication and new emerging applications. *Small* **2016**, *12*, 1400-1419, https://doi.org/10.1002/smll.201502988.

[20] Ma, X.; Ning, G.; Qi, C.; Xu, C.; Gao, J., Phosphorus and nitrogen dual-doped few-layered porous graphene: a high-performance anode material for lithium-ion batteries. *ACS Appl. Mater. Interfaces.* **2014**, *6*, 14415-14422, https://doi.org/10.1021/am503692g.

[21] Parambhath, V. B.; Nagar, R.; Ramaprabhu, S., Effect of nitrogen doping on hydrogen storage capacity of palladium decorated graphene. *Langmuir* **2012**, *28*, 7826-7833, https://doi.org/10.1021/la301232r.

[22] Gadipelli, S.; Guo, Z. X., Graphene-based materials: Synthesis and gas sorption, storage and separation. *Prog. Mater. Sci.* **2015**,*69*, 1-60, https://doi.org/10.1016/j.pmatsci.2014.10.004.

[23] Wang, L.; Lee, K.; Sun, Y. -Y.; Lucking, M.; Chen, Z.; Zhao, J. J.; Zhang, S. B., Graphene oxide as an ideal substrate for hydrogen storage. *ACS Nano* **2009**, *3*, 2995-3000, https://doi.org/10.1021/nn900667s.

[24] Das, M. R.; Sarma, R. K.; Saikia, R.; Kale, V. S.; Shelke, M. V.; Sengupta, P., Synthesis of silver nanoparticles in an aqueous suspension of graphene oxide sheets and its antimicrobial activity. *Colloids Surf. B: Biointerfaces* **2011**, *83*, 16-22, https://doi.org/10.1016/j.colsurfb.2010.10.033.

[25] Wang, Y.; Li, Z.; Wang, J.; Li, J.; Lin, Y., Graphene and graphene oxide: biofunctionalization and applications in biotechnology. *Trends Biotechnol.* **2011**, *29*, 205-212, https://doi.org/10.1016/j.tibtech.2011.01.008.

[26] Machado, B. F.; Serp, P., Graphene-based materials for catalysis. *Catal. Sci. Technol.* **2012**, *2*, 54-75, https://doi.org/10.1039/C1CY00361E.

[27] Bolotin, K. I.; Sikes, K. J.; Jiang, Z.; Klima, M.; Fudenberg, G.; Hone, J.; Kim, P.; Stormer, H., Ultrahigh electron mobility in suspended graphene. *Solid state Commun.* **2008**, *146*, 351-355, https://doi.org/10.1016/j.ssc.2008.02.024.

[28] Park, S.; Ruoff, R. S., Chemical methods for the production of graphenes. *Nat. Nanotechnol.* **2009**, *4*, 217-224, https://doi.org/10.1038/nnano.2009.58.

[29] Zhao, G.; Li, J.; Ren, X.; Chen, C.; Wang, X., Few-layered graphene oxide nanosheets as superior sorbents for heavy metal ion pollution management. *Environ. Sci. Technol.* **2011**, *45*, 10454-10462, https://doi.org/10.1021/es203439v.

[30] Fan, L.; Luo, C.; Sun, M.; Li, X.; Lu, F.; Qiu, H., Preparation of novel magnetic chitosan/graphene oxide composite as effective adsorbents toward methylene blue. *Bioresour. Technol.* **2012**, *114*, 703-706, https://doi.org/10.1016/j.biortech.2012.02.067.

[31] Ramesha, G.; Kumara, A. V.; Muralidhara, H.; Sampath, S., Graphene and graphene oxide as effective adsorbents toward anionic and cationic dyes. *J. Colloid Interface Sci.* **2011**, *361*, 270-277, https://doi.org/10.1016/j.jcis.2011.05.050.

[32] Chandra, V.; Kim, K. S., Highly selective adsorption of Hg^{2+} by a polypyrrole-reduced graphene oxide composite. *Chem. Comm.* **2011**, *47*, 3942-3944, https://doi.org/10.1039/C1CC00005E.

[33] Li, Y.; Zhang, P.; Du, Q.; Peng, X.; Liu, T.; Wang, Z.; Xia, Y.; Zhang, W.; Wang, K.; Zhu, H., Adsorption of fluoride from aqueous solution by graphene. *J. Colloid Interface Sci.* **2011**, *363*, 348-354, https://doi.org/10.1016/j.jcis.2011.07.032.

[34] Wang, J.; Chen, Z.; Chen, B., Adsorption of polycyclic aromatic hydrocarbons by graphene and graphene oxide nanosheets. *Environ. Sci. Technol.* **2014**, *48*, 4817-4825, https://doi.org/10.1021/es405227u.

[35] Chen, C.; Xu, K.; Ji, X.; Miao, L.; Jiang, J., Enhanced adsorption of acidic gases (CO_2, NO_2 and SO_2) on light metal decorated graphene oxide. *Phys. Chem. Chem. Phys.* **2014**, *16*, 11031-11036, https://doi.org/10.1039/C4CP00702F.

[36] Yi, Z.; Su, F.; Huo, L.; Cui, G.; Zhang, C.; Han, P.; Dong, N.; Chen, C., New insights into Li_2S_2/Li_2S adsorption on the graphene bearing single vacancy: A DFT study. *Appl. Surf. Sci.* **2020**, *503*, https://doi.org/10.1016/j.apsusc.2019.144446.

[37] Yu, J.; Hao, Z.; Wang, L.; Luo, Y.; Wang, J.; Sun, C.; Han, Y.; Xiong, B.; Li, H., First-principle calculations of adsorption of Ga (Al, N) adatoms on the graphene for the van-der-Waals epitaxy. *Mater. Today Commun.* **2021**, *26*, https://doi.org/10.1016/j.mtcomm.2020.101571.

[38] Rajivgandhi, G.; Rtv, V.; Nandhakumar, R.; Murugan, S.; Alharbi, N. S.; Kadaikunnan, S.; Khaled, J. M.; Alanzi, K. F.; Li, W. -J., Adsorption of nickel ions from electroplating effluent by graphene oxide and reduced graphene oxide. *Environ. Res.* **2021**, *199*, 111322-111322, https://doi.org/10.1016/j.envres.2021.111322.

[39] Sheng, L.; Ono, Y.; Taketsugu, T., *Ab initio* study of Xe adsorption on graphene. *J. Phys. Chem. C***2010**, *114*, 3544-3548, https://doi.org/10.1021/jp907861c.

[40] Ambrosetti, A.; Silvestrelli, P., Adsorption of rare-gas atoms and water on graphite and graphene by van der Waals-corrected density functional theory. *J. Phys. Chem. C* **2011**, *115*, 3695-3702, https://doi.org/10.1021/jp110669p.

[41] Maiga, S. M.; Gatica, S. M., Monolayer adsorption of noble gases on graphene. *Chem. Phys.* **2018**, *501*, 46-52, https://doi.org/10.1016/j.chemphys.2017.11.020.

[42] Vazhappilly, T.; Ghanty, T. K.; Jagatap, B., Adsorption properties of fission gases Xe and Kr on pristine and doped graphene: A first principle DFT study. *J. Nucl. Mater.* **2017**, *490*, 174-180, https://doi.org/10.1016/j.jnucmat.2017.04.017.

[43] Zhu, X.; Liu, K.; Lu, Z.; Xu, Y.; Qi, S.; Zhang, G., Effect of oxygen atoms on graphene: Adsorption and doping. *Phys. E: Low-dimens. Syst. Nanostructures* **2020**, *117*, 113827, https://doi.org/10.1016/j.physe.2019.113827.

[44] Qu, L. -H.; Fu, X. -L.; Zhong, C. -G.; Zhou, P. -X.; Zhang, J. -M., Equibiaxial Strained Oxygen Adsorption on Pristine Graphene, Nitrogen/Boron Doped Graphene, and Defected Graphene. *Materials* **2020**, *13*, 4945, https://doi.org/10.3390/ma13214945.

[45] Bagsican, F.R.; Winchester, A.; Ghosh, S.; Zhang, X.; Ma, L.; Wang, M.; Murakami, H.; Talapatra, S.; Vajtai, R.; Ajayan, P. M., Adsorption energy of oxygen molecules on graphene and two-dimensional tungsten disulfide. *Sci. Rep.* **2017**, *7*, 1-10, https://doi.org/10.1038/s41598-017-01883-1.

[46] Yan, H.; Xu, B.; Shi, S.; Ouyang, C., First-principles study of the oxygen adsorption and dissociation on graphene and nitrogen doped graphene for Li-air batteries. *J. Appl. Phys.* **2012**, *112*, 104316, https://doi.org/10.1063/1.4766919.

[47] Lee, K. -J.; Kim, S. -J., Theoretical investigation of CO_2 adsorption on graphene. *Bull. Korean Chem. Soc.* **2013**, *34*, 3022-3026, https://doi.org/10.5012/bkcs.2013.34.10.3022.

[48] Osouleddini, N.; Rastegar, S. F., DFT study of the CO_2 and CH_4 assisted adsorption on the surface of graphene. *J. Electron Spectros. Relate. Phenomena* **2019**, *232*, 105-110, https://doi.org/10.1016/j.elspec.2018.11.006.

[49] Takeuchi, K.; Yamamoto, S.; Hamamoto, Y.; Shiozawa, Y.; Tashima, K.; Fukidome, H.; Koitaya, T.; Mukai, K.; Yoshimoto, S.; Suemitsu, M., Adsorption of CO_2 on graphene: a combined TPD, XPS, and vdW-DF study. *J. Phys. Chem. C* **2017**, *121*, 2807-2814, https://doi.org/10.1021/acs.jpcc.6b11373.

[50] Tit, N.; Said, K.; Mahmoud, N. M.; Kouser, S.; Yamani, Z. H., *Ab-initio* investigation of adsorption of CO and CO_2 molecules on graphene: Role of intrinsic defects on gas sensing. *Appl. Surf. Sci.* **2017**, *394*, 219-230, https://doi.org/10.1016/j.apsusc.2016.10.052.

[51] Omidvar, A.; Mohajeri, A., Edge-functionalized graphene nanoflakes as selective gas sensors.

Sens. Actuators B Chem. **2014**, *202*, 622-630, https://doi.org/10.1016/j.snb.2014.05.136.

[52] Omidvar, A.; Mohajeri, A., Promotional effect of the electron donating functional groups on the gas sensing properties of graphene nanoflakes. *RSC Adv.* **2015**, *5*, 54535-54543, https://doi.org/10.1039/C5RA10298G.

[53] Tachikawa, H.; Yi, H.; Iyama, T.; Yamasaki, S.; Azumi, K., Hydrogen Storage Mechanism in Sodium-Based Graphene Nanoflakes: A Density Functional Theory Study. *Hydrogen* **2022**, *3*, 43-52, https://doi.org/10.3390/hydrogen3010003.

[54] Neese, F., The ORCA program system. *WIREs Comput. Mol. Sci.* **2012**, *2*, 73-78, https://doi.org/10.1002/wcms.81.

[55] Zhao, Y.; Truhlar, D. G., The M06 suite of density functionals for main group thermochemistry, thermochemical kinetics, noncovalent interactions, excited states, and transition elements: two new functionals and systematic testing of four M06-class functionals and 12 other functionals. *Theor. Chem. Acc.* **2008**, *120*, 215-241, https://doi.org/10.1007/s00214-007-0310-x.

[56] Akbari, E.; Namazian, M., Sulforaphane: A natural product against reactive oxygen species. *Comput. Theor. Chem.* **2020**, *1183*, 112850, https://doi.org/10.1016/j.comptc.2020.112850.

[57] Sviatenko, L. K.; Gorb, L.; Hill, F. C.; Leszczynska, D.; Okovytyy, S. I.; Leszczynski, J., Alkaline hydrolysis of hexahydro-1,3,5-trinitro-1,3,5-triazine: M06-2X investigation. *Chemosphere* **2015**, *134*, 31-38, https://doi.org/10.1016/j.chemosphere.2015.03.064.

[58] Sviatenko, L.; Gorb, L.; Leszczynska, D.; Okovytyy, S.; Shukla, M.; Leszczynski, J., In silico kinetics of alkaline hydrolysis of 1,3,5-trinitro-1,3,5-triazinane (RDX): M06-2X investigation. *Environ. Sci.: Processes. Impacts* **2017**, *19*, 388-394, https://doi.org/10.1039/C6EM00565A.

[59] Namazian, M.; Orangi, N.; Noorbala, M. R., Thermodynamic stability and structural parameters of carbon nanoclusters. *J. Theor. Comput. Chem.* **2014**, *13*, 1450058, https://doi.org/10.1142/S0219633614500588.

[60] Sert, Y.; Mahendra, M.; Shivashankar, K.; Puttaraju, K.; Doğan, H.; Çırak, Ç.; Ucun, F., Vibrational spectroscopy investigation using M06-2X and B3LYP methods analysis on the structure of 2-Trifluoromethyl-10H-benzo [4,5]-imidazo [1,2-a] pyrimidin-4-one. *Spectrochimica Acta A: Mol. Biomol. Spectros.* **2014**, *128*, 109-118, https://doi.org/10.1016/j.saa.2014.02.125.

[61] Vydrov, O. A.; Van Voorhis, T., Benchmark assessment of the accuracy of several van der Waals density functionals. *J. Chem. Theory Comput.* **2012**, *8*, 1929-1934, https://doi.org/10.1021/ct300081y.

[62] Reisi-Vanani, A.; Mehrdoust, S., Effect of boron doping in sumanene frame toward hydrogen physisorption: A theoretical study. *Int. J. Hydrog. Energy* **2016**, *41*, 15254-15265, https://doi.org/10.1016/j.ijhydene.2016.07.027.

[63] Rao, D.; Wang, Y.; Zhang, L.; Yao, S.; Qian, X.; Xi, X.; Xiao, K.; Deng, K.; Shen, X.; Lu, R., Mechanism of polysulfide immobilization on defective graphene sheets with N-substitution. *Carbon* **2016**, *110*, 207-214, https://doi.org/10.1016/j.carbon.2016.09.021.

[64] Wang, M.; Fan, X.; Zhang, L.; Liu, J.; Wang, B.; Cheng, R.; Li, M.; Tian, J.; Shi, J., Probing the role of O-containing groups in CO_2 adsorption of N-doped porous activated carbon. *Nanoscale* **2017**, *9*, 17593-17600, https://doi.org/10.1039/C7NR05977A.

[65]Kasuriya, S.; Namuangruk, S.; Treesukol, P.; Tirtowidjojo, M.; Limtrakul, J., Adsorption of ethylene, benzene, and ethylbenzene over faujasite zeolites investigated by the ONIOM method. *J. Catal.* **2003**, *219*, 320-328, https://doi.org/10.1016/S0021-9517(03)00213-6.

[66] Zhu, Y. -q.; Su, H.; Jing, Y.; Guo, J.; Tang, J., Methane adsorption on the surface of a model of shale: A density functional theory study. *Appl. Surf. Sci.* **2016**, *387*, 379-384, https://doi.org/10.1016/j.apsusc.2016.06.033.

[67] Izgorodina, E. I.; Brittain, D.R.; Hodgson, J. L.; Krenske, E. H.; Lin, C. Y.; Namazian, M.; Coote, M. L., Should contemporary density functional theory methods be used to study the thermodynamics of radical reactions? *J. Phys. Chem. A* **2007**, *111*, 10754-10768, https://doi.org/10.1021/jp075837w.

[68] Atkins, P. W.; De Paula, J., *Physical chemistry*. Oxford university press: **1998**.